# PROCEEDINGS OF THE 16th SYMPOSIUM ON THE GEOLOGY OF THE BAHAMAS AND OTHER CARBONATE REGIONS

**Edited by**
**Bosiljka Glumac and Michael Savarese**

Gerace Research Centre
San Salvador, Bahamas

2016

Cover photo: San Salvador coastline photo by Erin Rothfus.

Press:  A & A Printing

# BIOSTRATIGRAPHIC AND GEOCHEMICAL EVIDENCE FOR A TECTONICALLY INDUCED CHANGE IN THE AGGRADATION RATE OF THE MAYAGUANA BANK (SE BAHAMAS) DURING THE EARLY MIOCENE

Gyöngyvér Fischer[*], Fabienne Godefroid, Pascal Kindler, and Erika Baldessin

Section of Earth and Environmental Sciences, University of Geneva, 1205 Geneva, Switzerland

**ABSTRACT.** Preliminary biostratigraphic and geochronological results obtained from a 44 m-long core drilled on the northern coast of Mayaguana Island (SE Bahamas) show that the topmost layers of the core date from the Burdigalian (Early Miocene), whereas the deepest units are of Chattian (Late Oligocene) or Aquitanian (Earliest Miocene) age. Accordingly, the platform aggraded 44 m of sediments in a 10 to 3 my time span, from the Chattian/Aquitanian to the Burdigalian, whereas previous surface investigations of the island showed that only 11 m of carbonates were accumulated in a 17 my-long period, between the Burdigalian and the Early Pleistocene. This new record shows that the accumulation rate of the Mayaguana Bank was much higher during the Late Paleogene/Early Miocene than during the time interval from the Middle Miocene to the Pleistocene. This decrease is likely due to vertical tectonic motions related to the late phases of the Cuban orogeny which reduced accommodation on the platform top. These results designate the Mayaguana Bank as an accurate gauge to record the elevation of sea-level highstands during the Neogene.

[*]Corresponding author. E-mail: Gyongyver.Fischer@unige.ch

## INTRODUCTION

Because photozoan carbonates tend to keep up with sea level and because they are very sensitive to subtle environmental changes (Schlager 2000; 2005), investigating the anatomy of tropical platforms is a powerful means to unravel regional tectonic evolution and trace basin-wide and/or global climatic changes. The problem lies in the difficulty of disentangling the relative importance of tectonic *versus* climatic factors on carbonate sediment accumulation.

Our present research aims to explore the subsurface geology of the Mayaguana Bank through three scientific cores drilled on the north coast of Mayaguana Island, and twelve industrial cores drilled in its southern part. Core depths range between 16.8 and 44.2 m below the island surface (mbis). These cores will provide evidence to refine our understanding of the geologic and tectonic history of this bank, and to better

constrain regional to global sea-level and climatic fluctuations during the Late Cenozoic. This paper presents the preliminary results obtained from the bottom portion of the 44.2 m-deep core drilled at the western end of the Little Bay headland (the Core-LB), along the northern shoreline of Mayaguana where karstified limestones of Burdigalian (Early Miocene) age are exposed (Godefroid, 2012).

## SETTING

### The Bahamas Archipelago

The Bahamas (Commonwealth of the Bahamas; Figures 1 and 2) is a NW-SE trending archipelago located in the Northwestern Atlantic Ocean. It extends over more than 1'400 km (Pierson, 1982) from off the coast of Florida to the northern tip of Hispaniola including the Bahama Banks, the Turks and Caicos Platforms (British West Indies) and the submerged Mouchoir, Silver,
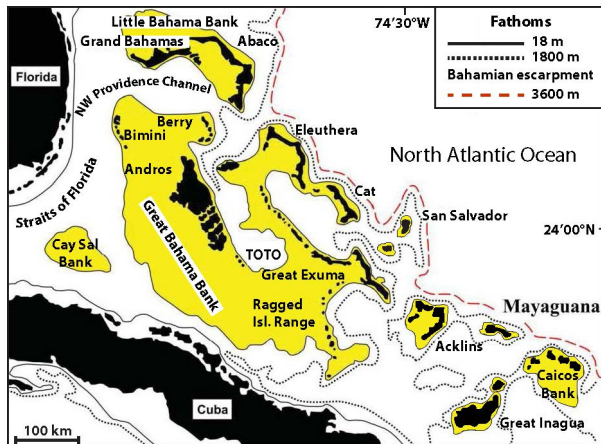
*Figure 1. Map of The Bahamas showing the location of the Mayaguana platform. Map modified from Godefroid (2012).*
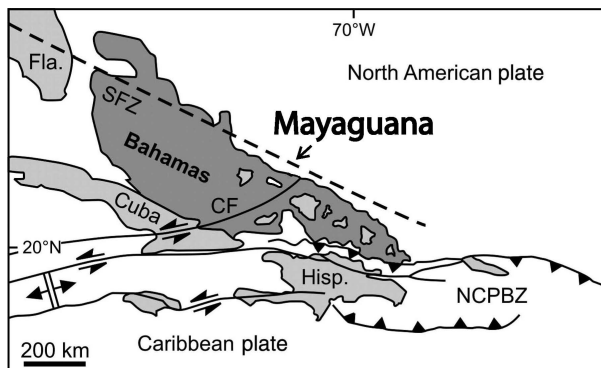


*Figure 2. Tectonic setting of the study area (arrow) modified from Kindler et al. (2011). Fla. = Florida, Hisp. = Hispaniola, NCPBZ = North Caribbean plate boundary zone, SFZ = Sunniland fracture zone, and CF =Cauto fault.*

and Navidad Banks. The archipelago stands on the passive margin of the North American plate, but in close proximity to the tectonically active North Caribbean plate boundary zone (Figure 2). It parallels also the N60°W-trending Sunniland fracture zone, which is related to the Jurassic rifting phase of the North Atlantic Ocean (James, 2009), and it is cross cut by the NE extension of the sinistral, and still active, strike-slip Cauto fault, which stretches out through the Caicos passage (Meyerhoff and Hatten, 1974; Cotilla Rodriguez et al., 2007).

### The Mayaguana Bank

Located in the southeastern portion of the Bahamas, the Mayaguana Bank is a small elongated (53x12 km), E-W trending carbonate platform capped by a low relief island covering most of its area (Figure 3; Pierson, 1982; Godefroid, 2012). The platform emerges from the same 2000 m depth contour as the Crooked-Acklins Platform situated ~80 km towards the NW and is separated from the Caicos Bank, ~65 km to the SE, by the deep Caicos passage (Figure 2; Meyerhoff and Hatten, 1974; Kindler et al., 2011).
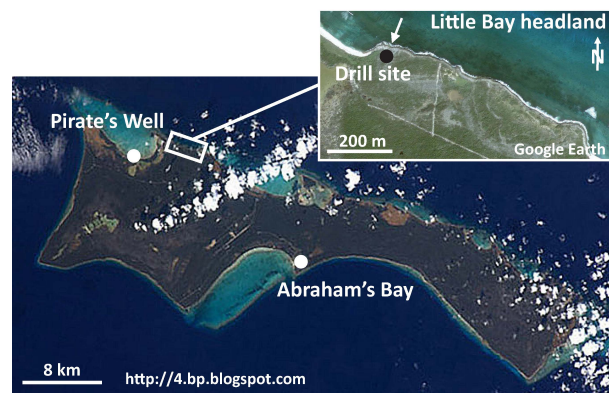


*Figure 3 Aerial view of the Mayaguana Bank and location of the drill site.*

### Mayaguana Island

Due to its relative inaccessibility, Mayaguana Island received little attention from scientists before the 21ˢᵗ century. It was first studied by Cant (1977) who mainly focused on the fossil bank-barrier reef riming most of the island. Pierson (1982) and later Vahrenkamp et al. (1991) examined Cenozoic carbonates obtained from shallow cores drilled by the Bahamian Ministry of Work and Utilities, and by the United States Geological Survey (Klein, 1958). In recent times, an extensive geological study of Mayaguana Island was made by scientists from the University of Geneva (Kindler et al., 2008, 2011; Godefroid, 2012), who first reported outcrops of shallow-water carbonates of Miocene, Pliocene, and Early Pleistocene age on the north coast of the island, invalidating the assumption that the Bahamian

islands expose no older rocks than the Middle Pleistocene (Carew and Mylroie, 1995; Mylroie, 2008; Hearty and Kaufman, 2000). In the SE Bahamas, carbonates of Pliocene age had only been previously reported by Pierson (1982) at depths of several tens of meters, with the shallowest occurrence reached at ~9 m below the surface in the southern part of Mayaguana. This discovery suggests a more complex and independent tectonic history of the Mayaguana Platform with respect to the other banks from the southeastern part of the Bahamas archipelago (Pierson, 1982; Kindler et al., 2008, 2011; Godefroid, 2012).

The study area is situated along the north coast of Mayaguana, at the western end of the Little Bay headland which comprises a succession of distinctive rock units, biostratigraphically and geochemically dated from the Burdigalian to the Early Pleistocene (Figure 3; Kindler et al., 2011; Godefroid, 2012).

*Island Stratigraphy*

Mayaguana Island exposes peritidal carbonates deposited during interglacial sea-level highstands separated by paleosols and/or karstic surfaces formed during glacial sea-level lowstands. Eight main lithostratigraphic units occur on the island spanning the Burdigalian (Early Miocene) to the Holocene (Godefroid, 2012). The four younger lithostratigraphic units, from the Middle Pleistocene to the Holocene, are present across the whole island and are well known on other Bahamian islands (Carew and Mylroie, 1995; Kindler and Hearty, 1996; Hearty and Kaufman, 2000; Kindler et al., 2007, 2010). The four older units, from the Burdigalian to the Early Pleistocene, are reported exclusively from Mayaguana Island and are restricted to its north coast. The youngest Quaternary units (Rice Bay, Whale Point, Grotto Beach, and Owl's Hole Formations) consist of skeletal and peloidal-oolitic carbonate sands mainly deposited in intertidal to supratidal settings. One important exception is the

Grotto Beach Formation which comprises shallow subtidal, lagoonal, and reefal facies (e.g., Chen et al., 1991). The four Neogene to Early Quaternary units include well-indurated skeletal limestones and dolostones representing reefal, lagoonal, and beach deposits. Their main characteristics are briefly summarized below based on Godefroid (2012).

The Mayaguana Formation. This unit, further described in Godefroid (this volume), consists of a hard, bioclastic limestone rich in larger benthic foraminifera characteristic of a shallow-water, peri-reefal setting. In particular, *Miogypsina* cf. *intermedia*, *M. globulina* and *Miolepidocyclina* cf. *burdigalensis* have been identified indicating an Early Miocene, Burdigalian age (see Plate I/11 and 13). Mean $^{87}Sr/^{86}Sr$ ratios are $0.708546 \pm 0.00001$ supporting the Burdigalian biostratigraphic age (18.4 - 18.7 Ma).

The Little Bay Formation. This unit forms three small outcrops along the Little Bay headland, two at its extremities and one approximately halfway in between, at elevations from present sea-level up to +1.5 m. It consists of a finely laminated, porcelain white, microsucrosic dolostone. Tide-generated sedimentary structures such as multi-directional cross-bedding and ripple laminations are visible, implying that this unit was deposited in a high-energy tidal environment. The $^{87}Sr/^{86}Sr$ ratios average at $0.708988 \pm 0.000025$ indicating a Late Miocene, Messinian age (5.59-6.81 Ma).

The Timber Bay Formation. This unit is common along the north coast of Mayaguana Island where it forms narrow but extensive outcrops exposed at elevations between present sea-level and +3.0 m. It consists of a well-lithified, massive, bioclastic dolostone rich in corals and encrusting organisms (red algae and benthic foraminifera) forming coralgal build-ups. Fine cryptocrystalline dolomite replaces the allochems while coarse crystals fill the intergranular and intragranular pore spaces. The

coralgal framestones indicate a shallow-water, high-energy reefal environment. The mean $^{87}Sr/^{86}Sr$ ratios are 0.709067 ± 0.000011 corresponding to the Middle Pliocene, Zanclean to the Early Gelasian age (2.12-4.09 Ma).

The Misery Point Formation. This formation is exposed at several locations along the north coast of the island at elevations from present sea-level up to +12 m. The most striking exposure is the Misery Point Cliff which constitutes a one km-long and 12 m-thick outcrop. The Misery Point Formation comprises three vertically stacked lithostratigraphic units (members) separated by paleosols and/or marine erosional surfaces. They consist of coarse- to fine-grained bioclastic grainstones. From base to top, these units are characteristic of reefal, lagoonal, and beach environments, respectively. The $^{87}Sr/^{86}Sr$ ratios range from 0.709126 ± 0.000008 to 0.709138 ± 0.000015 indicating an Early Pleistocene, Calabrian age (~1.0-1.19 Ma).

METHODS

*Drilling*

A Central Mine Equipment 750X rubber-tired core drill (Figure 4) was conveyed on recent sands, near the karstified surface of the Mayaguana Formation on the Little Bay headland (Figure 5) in mid-November 2011. This drilling site (N22°26.531', W73°03.790') was selected because it is the closest locale to the top of the Mayaguana Formation (Figure 5) with the aim to recover the oldest possible rocks from the subsurface. Once the drill and the water pump were set up, the technicians proceeded to drill through the soft recent material with an auger drill (helical screw) until they hit the bedrock. Afterwards, the auger was removed and casing was placed in the hole to prevent modern sediment from falling into it. Water was pumped directly from the ocean and used to cool the drilling bit. A 10 cm-diameter hole was drilled with a surface-set diamond coring bit on a HQ inner core barrel



*Figure 4. Central Mine Equipment 750X rubber-tired core drill at the study site.*
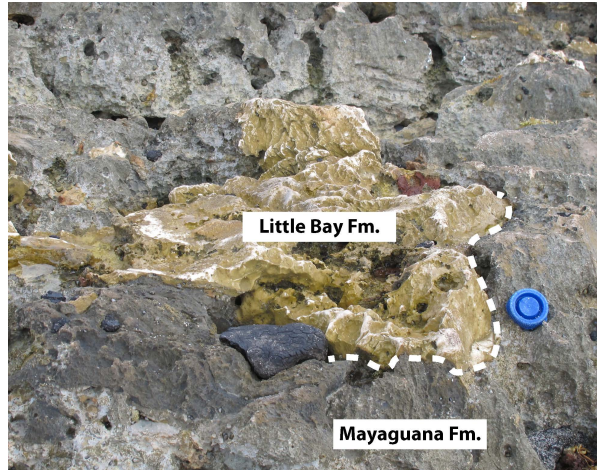


*Figure 5. Karstified surface at Little Bay showing the contact (dotted line) between the Mayaguana and the Little Bay Formations. Diameter of the bottle cap = 2 cm.*

(Figure 6) to obtain a 6.3 cm-diameter core. The barrels measure approximately 3 m in length (5 feet), so every 3 m a new drill rod was added to continue drilling down into the bedrock. When we ran out of rods, the core pieces were retrieved, measured, and stored in cardboard boxes (Figure 6). At this site, a depth of 44.2 mbis (~41 m below mean sea level) was reached with a recovery close to 100%. Due to time constraints, the core was not directly logged in the field, but each core piece was measured and labelled to

*Figure 6. 10 cm-diameter drill bit with 6.3 cm-diameter core pieces stored in a cardboard box. A) Surface-set diamond coring bit and HQ core barrels, scale in inches. B) Core pieces showing the karstified Mayaguana Formation between 2.80 m below the island surface (mbis) and 4.42 mbis.*

ensure its original position and orientation, and thus prevent any loss of information between the drilling site and the laboratory in Geneva. Nonetheless, the lowermost 21 cm-long portion of the core (Figure 7) was brought back for petrographic and geochemical analyses, while the rest of the core remained on Mayaguana waiting for shipment. This 21 cm-long core piece represents the baseline data for this paper.

### Biostratigraphic and Sr-isotope Analyses

A one-cm thick slab, destined for thin section preparation, was cut out of the length of the core piece, while the two remaining halves were polished and examined with a hand lens. Four large (6.0 x 4.5 cm) oriented thin sections were made and examined with a petrographic microscope to study the assemblages of benthic foraminifera. Foraminifer identification was performed with the help of Prof. Roland Wernli and Dr. Seyedabolfalz Hosseini (University of Geneva).

Two whole-rock samples from the core slab, approximately 1 cm$^3$ in volume, were crushed with an agate mortar to obtain a flour fine powder. For each sample, 0.03 g of powder was collected in plastic tubes for multiphasic leaching. To extract and purify the strontium, samples were first bathed in 1.5 mL of 2.2 M concentration

acetic acid and left to rest until all the carbonates were dissolved (~1 hour). The solution containing the residue was then poured out into centrifuge tubes and centrifuged for 20 minutes. The residue was separated from the solvent, decanted into plastic tubes, and bathed a second time in 1.5 mL of acetic acid (2.2 M). Once the acid was completely evaporated (~2 hours) a few drops of nitric acid (15 M) were added. The strontium was extracted through column chromatography (Still et



*Figure 7. View of the retrieved basal core piece from 43.07 mbis to 43.30 mbis. White arrows indicate rhizoliths; black arrow shows the geopetal infill of a dissolution void.*

al., 1978; Harwood and Moody, 1989; Fair and Kormos, 2008) and measured with a Thermal Ionization Mass Spectrometer Finnigan NEPTUNE with an intrinsic error of 9 ppm (1 σ = 0.000009). The $^{87}Sr/^{86}Sr$ values were internally corrected for instrumental mass fractionation using a $^{88}Sr/^{86}Sr$ value of 8.375209. All Sr-isotope ratios presented in this study were further corrected for external fractionation by normalization to the given value of the SRM987 standard ($^{87}Sr/^{86}Sr$ = 0.710248). Numerical ages were then obtained by comparison with the Sr-isotope evolution of global seawater for the Neogene reported as the look-up table Version 4:08/04 (Howarth and McArthur, 1997; McArthur et al. 2001).

The reliability of bulk-rock sample analyses in Sr-isotope stratigraphy is controversial. Indeed, measured values correspond to an average of $^{87}Sr/^{86}Sr$ ratios from the rock particles and matrix, as well as from the diagenetic alteration products, such cements and pedogenic features. The lack of large, well-preserved bioclasts in the studied core slab did not allow us to avoid this problem, but we paid particular attention to select the most pristine rock chips for crushing. Accordingly, we consider our Sr ratios as indicating the youngest possible age of the rocks, despite the fact that, for the Mayaguana Formation (Godefroid, 2012), there is a perfect correlation between radiometric and biostratigraphic ages.

<center>RESULTS</center>

The studied core piece consists of a fine-grained, light brown, slightly pedogenised bioclastic limestone (Figure 7) containing rhizoliths and few, cm-sized dissolution voids partially infilled by white, geopetal microsucrosic dolostone (Figure 7, black arrow). Microfacies analysis reveals a poorly sorted packstone/grainstone containing numerous red algae, mollusc, and coral fragments (Figure 8), and a rich assemblage of hyaline and porcelaneous benthic foraminifera including *Praerhapydionina delicata*
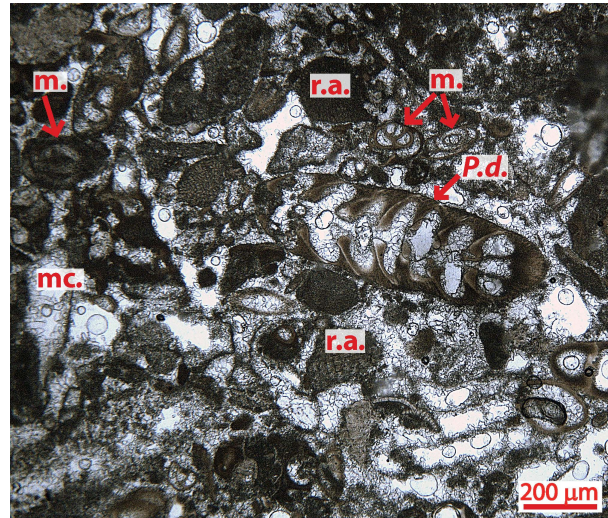


*Figure 8. Microfacies from the bottom 21 cm of the LB core showing a bioclastic packstone/grainstone with* Praerhapydionina delicata *(P.d.), miliolids (m.), red algae (r.a.), and mollusc (mc.) molds.*

(Plate I/1-2), *Peneroplis* aff. *thomasi* (Plate I/5), *Archaias* aff. *operculiniformis* (Plate I/4), *A.* cf. *kirkukensis* (Plate I/3), *Spirolina cylindracea* (Plate I/6), *Dendritina* sp. (Plate I/9), *Planorbulina* sp. (Plate I/12), *Neorotalia lithothamnica* (Plate I/7-8), and *N. viennotti* (Plate I/10). The aforementioned benthic foraminifera characterize low- to moderate-energy settings in lagoonal to peri-reefal environments (Robinson and Wright, 1993; Cahuzac and Poignant, 1997; Sirel, 2003; Bassi et al., 2007; BouDagher-Fadel, 2008; Ahmadi and Motaharian, 2010). The $^{87}Sr/^{86}Sr$ ratios, obtained from whole-rock samples, range between 0.708358 ± 0.000004 and 0.708396 ± 0.000004.

<center>DISCUSSION</center>

<center>*Age of the Core Base*</center>

Reliable biostratigraphic markers for the Oligocene to Early Miocene time interval such as miogypsinids and nummulitids are not present in the studied samples. Miogypsinids are known in the American Province from the Early Oligocene (Rupelian, Eames et al., 1968; BouDagher-Fadel and Price, 2010) to the Late-Early Miocene

<center>6</center>

(Burdigalian, BouDagher-Fadel, 2008; BouDagher-Fadel and Price, 2013), whereas nummulitids (*sensu stricto*) are known from the Paleocene to the Early Oligocene (Rupelian, Adams, 1967; Cahuzac et Poignant, 1997; Serra-Kiel et al., 1998; BouDagher-Fadel, 2008). These foraminifera flourish in shallow-water, tropical to subtropical seas in high-energy reefal settings (Serra-Kiel et al., 1998; BouDagher-Fadel, 2008, 2010, 2013), thus their absence can be explained by the low- energy depositional environment of the studied core piece. The observed hyaline and porcelaneous benthic foraminifera are less reliable for biostratigraphy. The most dependable taxon is *Praerhapydionina delicata* (Plate I/1-2) which was identified in our thin sections. In the American realm, *P. delicata* is restricted to the Oligocene, whereas its stratigraphic range includes the Earliest Miocene in the Middle East, Far East, North Africa and Europe (Rupelian-Aquitanian; Eames et al., 1962; Henson, 1950; Robinson and Wright, 1993). Granier et al. (2013) illustrate sections of *Pseudorhapydionina moulladei* in well-dated Paleocene lithologies from Guatemala which are confusingly similar to our sections of *P. delicata*. The main diagnostic criteria to differentiate these two species are the juvenile stage and the aperture(s). *Pseudorhapydionina moulladei* has a biserial juvenile stage and a cribrate aperural face in the uniserial adult stage (Pécheux, 1995), while *P. delicata* has a planispiral juvenile stage and a stellate terminal aperture in the uniserial adult stage (Henson, 1950). The specimen illustrated in Plate I/1 shows no evidence of a cribrate apertural face, nor of a biserial juvenile stage. Therefore, we assume that our determinations are correct and that this species is *P. delicata*. In addition, the presence of *Archaias* aff. *operculiniformis* (Plate I/4) and *A.* cf. *kirkukensis* (Plate I/3) could indicate a Chattian age (28.1 to 23.0 Ma; Smout and Eames, 1958; Eames et al., 1962) for the bottom of Core-LB. In contrast, numerical ages obtained by Sr-isotope stratigraphy (Howarth and McArthur, 1997;

McArthur et al. 2001) indicate, for the same samples, an age between 21.53 and 20.79 Ma BP, corresponding to the Aquitanian.

The moderate agreement between biostratigraphic and Sr ages obtained from our samples can be explained in two ways: (1) subaerial weathering and pedogenic processes, which left an imprint on our core piece (Figures 7 and 8), could have shifted Sr ratios towards higher values (i.e. towards a younger age; Capo et al., 1998; Stewart et al., 1998) or, alternatively, (2) *A.* aff. *operculiniformis*, which possibly constrains the age of our samples to the Late Oligocene, could have a longer extension on the Mayaguana Bank than elsewhere, or it could have been mistaken with a younger species of this genus. In any case, we can safely assume that the age of the lowermost portion of our core ranges between the Late Oligocene (Chattian) and the Earliest Miocene (Aquitanian), i.e. between 28.1 and 20.8 Ma.

*Accumulation Rates of the Mayaguana Bank*

Accumulation rates of carbonate platforms are obtained by dividing sediment thickness by interval duration (Bosscher and Schlager, 1993). According to Bosscher and Schlager (1993) the accumulation rates of Phanerozoic carbonate edifices, not taking into account sediment compaction, average at 100 m/my, with a maximum accumulation rate up to 200 m/my. In addition, accumulation rates tend to decrease when the sampling interval increases, possibly because of the more frequent occurrence of intervals of non-deposition (Bosscher and Schlager, 1993; Schlager, 1999). More specifically, accumulation rates calculated for Cenozoic platforms in the vicinity of the Mayaguana Bank range between 48 and 11 m/my, with sampling intervals comprised between 65.0 and 1.5 Ma (Table 1). Finally, according to Godefroid (2012), 11 m of shallow-water carbonates were accumulated on the Mayaguana Bank between the Burdigalian and the Early Pleistocene, which corresponds to a mean

| Platform | Time interval | Mean rate | Reference |
|---|---|---|---|
| | (Ma) | (m/my) | |
| Turks and Caicos | 38-0 | 47.4 | Bosscher and Schlager, 1993 |
| Andros Island | 38-0 | 17.6 | Bosscher and Schlager, 1993 |
| Long Island | 65-0 | 18.8 | Bosscher and Schlager, 1993 |
| Little Bahama Bank | 5.0-2.0 | 11-14 | McNeill, 2005 |
| Great Bahama Bank | 3.5-2.0 | 17-20 | McNeill, 2005 |
| San Salvador | 4.5-2.0 | 26 | McNeill, 2005 |
| Mayaguana Island | 18.7-1.0 | 0.6 | Godefroid, 2012 |
| Mayaguana Bank | 21.5-1.0 | 2.5 | this paper |
| Mayaguana Bank | 28.1-1.0 | 1.9 | this paper |
| Core-LB | 21.5-18.7 | 15.8 | this paper |
| Core-LB | 28.1-18.7 | 4.7 | this paper |

*Table 1.  Accumulation rates of Cenozoic carbonate platforms in the Bahamas area from the literature and the present paper.*

aggradation rate of 0.6 m/my (11 m / 17 my; Table 1).

Combining our data with those of Godefroid (2012), we can calculate a mean accumulation rate of 1.9 or 2.5 m/my on the Mayaguana Bank for the time interval from the Chattian to the Early Pleistocene, or respectively, from the Aquitanian to the Early Pleistocene (Table 1).  Focusing on the 44 m-long Core-LB, and knowing that rocks from the core top are of Burdigalian age (18.4 to 18.7 Ma; Godefroid, 2012), we obtain an accumulation rate of 4.7 m/my and, respectively 15.8 m/my, depending on whether the base of the core is Chattian or Aquitanian in age (Table 1).  Varying with the exact age of the core base (Aquitanian or Chattian), carbonate accumulation rate on the Mayaguana Bank could therefore have been similar (ca. 15 m/my), or significantly lower (ca. 5 m/my) around the Paleogene/Neogene boundary with respect to neighbouring Bahamian platforms (Table 1).  In any case, the aggradation rate dropped dramatically to approximately 0.6 m/my on this platform in the time interval from the Burdigalian to the Early Pleistocene (18.7-1.0 Ma; Godefroid, 2012).  Accumulation rates hinge on the growth potential of carbonate systems and the available accommodation, which is itself mostly controlled by regional tectonics and glacio-

eustasy.  To our knowledge, with the possible exception of the extinction of miogypsinids in the Late Burdigalian (ca. 16 Ma; BouDagher-Fadel and Price, 2013), no major biotic crisis, that could explain the decrease in accumulation rate on the Mayaguana Bank, occurred in the Caribbean realm during the Miocene.  Therefore, this change could be related either to regional tectonics, or to glacial eustasy, or to a combination of both of these controlling factors.  Accommodation could have been reduced from the Burdigalian onwards because of strike-slip faulting and minor deformations associated with vertical oscillatory movements along the Cuban neo-autochthon (Iturralde-Vinent, 1994; James, 2009).  Alternatively, or concurrently, accumulation rate could have been lowered due to increased episodes of platform emergence and denudation related to the inception of Antarctic glaciations in the Early Miocene (Pekar and DeConto, 2006).  Because neighbouring carbonate platforms (e.g., San Salvador, Great Bahama Bank, Little Bahama Bank) did not experience changing aggradation in the Neogene (Table 1; McNeill, 2005), we conclude that regional tectonic activity, namely a halt in subsidence was instrumental in reducing, by a factor of 10 to 30, the accumulation rate on the Mayaguana Bank from the Burdigalian onwards.

## CONCLUSIONS

Biostratigraphic and geochronological data obtained from the base of a 44 m-long core drilled on Mayaguana Island (SE Bahamas) and from exposures near the drilling site show that the carbonate accumulation rate dropped dramatically on this platform from values estimated between 5 and 15 m/my in the Late Oligocene/Earliest Miocene to ca. 0.6 m/my for the time interval from the Burdigalian to the Early Pleistocene. Because neighbouring Bahamian platforms did not record this change in aggradation, we surmise that it is related to tectonic action restricted to the Mayaguana region. Transpressive motion along adjacent strike-slip faults could have halted the bank subsidence since the Burdigalian. If confirmed, these conclusions would designate the Mayaguana Bank as a perfect gauge to record the elevation of sea-level highstands during the Neogene. Ongoing investigations of the other cores recently retrieved from Mayaguana Island will certainly contribute to refine the conclusions drawn from the present research.

## ACKNOWLEDGMENTS

## REFERENCES

Adams, C.G., 1967, Tertiary Foraminifera in the Tethyan, American, and Indo-Pacific Provinces, *in* Adams, C.G., Ager, D., eds., Aspects of Tethyan biogeography: Systematics Association Publication, London, Special Publication, v. 7, p. 195-217.

Ahmadi, V., and Motaharian, A., 2010, Microbiostratigraphy and paleoecology of benthic foraminifers study based on the microfacies and sedimentary sequence identification and interpretation in Asmari Formation of South- East of Shiraz (Fars province): The First International Applied Geological Congress, Iran, p. 885-890.

Bassi, D., Hottinger, L., and Nebelsick, J.H., 2007, Larger foraminifera from the Upper Oligocene of the Venetian area, north-east Italy: Palaeontology, v. 50, p. 845-868.

Bosscher, H., and Schlager, W., 1993, Accumulation rates of carbonate platforms: The Journal of Geology, v. 101, p. 345-355.

BouDagher-Fadel, M.K., 2008, Evolution and geological significance of larger benthic foraminifera: Developments in Palaeontology and Stratigraphy, v. 21, p. 1-540.

BouDagher-Fadel, M.K., and Price, G.D., 2010, American Miogypsinidae: An analysis of their phylogeny and biostratigraphy: Micropaleontology, v. 56, p. 567-586.

BouDagher-Fadel, M.K., and Price, G.D., 2013, The phylogenetic and palaeogeographic evolution of the miogypsinid larger benthic foraminifera: Journal of the Geological Society, v. 170, p. 185-208.

Cant, R.V., 1977, Role of coral deposits in building the margins of the Bahama Banks: Proceedings of the

Third International Coral Reef Symposium, Miami, Florida, v. 2, p. 9-13.

Cahuzac, B., and Poignant, A., 1997, Essai de biozonation de l'Oligo-Miocène dans les bassins européens à l'aide des grands foraminifères néritiques: Bulletin de la Société Géologique de France, v. 168, p. 155-169.

Capo, R.C., Stewart, B.W., and Chadwick, O.A., 1998, Strontium isotopes as tracers of ecosystem processes: theory and methods: Geoderma, v. 82, p. 197–225.

Carew, J.L., and Mylroie, J.E., 1995, Depositional model and stratigraphy for the Quaternary geology of the Bahama Islands, *in* Curran, H.A., and White, B., eds., Terrestrial and shallow marine geology of the Bahamas and Bermuda: Geological Society of America, Special Paper, v. 300, p. 5-32.

Chen, J.H., Curran, H.A., White, B., and Wasserburg, G.J., 1991, Precise chronology of the last interglacial period: $^{234}$U-$^{230}$Th data from fossil coral reefs in the Bahamas: Geological Society of America Bulletin, v. 103, p. 82-97.

Cotilla Rodriguez, M.O., Franzke, H.J., and Cordoba Barba, D., 2007, Seismicity and seismoactive faults of Cuba: Russian Geology and Geophysics, v. 48, p. 505-522.

Eames, F.E., Banner, F.T., Blow, W.H., and Clarke, W.J., 1962, Fundamentals of Mid-Tertiary Stratigraphical Correlation: Cambridge University Press, 163 p.

Eames, F.E., Clarke, W.J., Banner, F.T., Smout, A.H., and Blow, W.H., 1968, Some larger foraminifera from the Tertiary of Central America: Palaeontology, v. 11, p. 49-59.

Fair, J.D., and Kormos, Ch.M., 2008, Flash column chromatograms estimated from thin-layer chromatography data: Journal of Chromatography A, v. 1211, p. 49-54.

Godefroid, F., 2012, Géologie de Mayaguana, SE de l'archipel des Bahamas: Terre & Environnement, v. 108, 230 p.

Granier, B., Radoičić, R., and Drobne, K., 2013, Revision of the Jesse Harlan JOHNSON Collection. Part 1. Some fossil Dasycladales from Guatemala: Carnets de Géologie [Notebooks on Geology], Brest, Article 2013/07 (CG2013_A07), p. 281-301.

Harwood, L.M., and Moody, C.J., 1989, Experimental Organic Chemistry: principles and practice: Oxford, Blackwell, 778 p.

Hearty, P.J., and Kaufman, D.S., 2000, Whole-rock aminostratigraphy and Quaternary sea-level history of the Bahamas: Quaternary Research, v. 54, p. 163-173.

Henson, F.R.S., 1950, Middle Eastern Tertiary Peneroplidae (Foraminifera), with remarks on the phylogeny and taxonomy of the family: Thesis, West Yorkshire Printing Co. Limited Publication, Leiden, Wakefield England, v. 19, 70 p.

Howarth R.J., and McArthur J.M., 1997, Statistics for strontium isotope stratigraphy. A robust LOWESS fit to the marine Sr-isotope curve for 0 - 206 Ma, with look-up table for the derivation of numerical age: Journal of Geology, v. 105, p. 441-456.

Iturralde-Vinent, M.A., 1994, Cuban geology: a new plate-tectonic synthesis: Journal of Petroleum Geology, v. 17, p. 39-70.

James, K.H., 2009, Evolution of Middle America and the *in situ* Caribbean plate model, *in* James, K.H., Lorente, M.A., and Pindell, J.L., eds., The origin and evolution of the Caribbean plate: Geological Society of London, Special Publication, v. 328, p. 127-138.

Kindler, P., Godefroid, F., Chiaradia, M., Ehlert, C., Eisenhauer, A., Frank, M., Hasler, C.-A., and Samankassou, E., 2011, Discovery of Miocene to early Pleistocene deposits on Mayaguana, Bahamas: Evidence for recent active tectonism on the North American margin: Geology, v. 39, p. 523-526.

Kindler, P., Godefroid, F., and Samankassou, E., 2008, Pre-Holocene island geology of the Caicos and Mayaguana (Bahamas) Platforms: similarities and differences: Society for Sedimentary Geology, SEPM Core Workshop, v. 22, p. 211-213.

Kindler, P., and Hearty, P.J., 1996, Carbonate petrography as an indicator of climate and sea-level changes: new data from Bahamian Quaternary units: Sedimentology, v. 43, p. 381-399.

Kindler, P., Mylroie, J.E., Curran, H.A., Carew, J.L., Gamble, D.W., Rothfus, T.A., Savarese, M., and Sealey, N.E., 2010, Geology of Central Eleuthera, Bahamas: a field trip guide: Fieldtrip guidebook,

The 15th Symposium on the Geology of the Bahamas and Other Carbonate Regions, Gerace Research Centre, San Salvador Island, Bahamas, 75 p.

Kindler, P., Reyss, J.-L., Cazala, C., and Plagnes, V., 2007, Discovery of a composite reefal terrace of middle and and late Pleistocene age in Great Inagua Island, Bahamas: Implications for regional tectonics and sea-level history: Sedimentary Geology, v. 194, p. 141-147.

Klein, H., Hoy, N.D., and Sherwood, C.B., 1958, Geology and ground-water resources in the vicinity of the Auxiliary Air Force Bases, British West Indies: U.S. Geological Survey open-file report, 142 p.

McArthur, J.M., Howarth, R.J., and Bailey, T.R., 2001, Strontium isotope stratigraphy: LOWESS Version 3. Best-fit line to the marine Sr-isotope curve for 0 to 509 Ma and accompanying look-up table for deriving numerical age: Journal of Geology, v. 109, p. 155-169.

McNeill, D.F., 2005, Accumulation rates from well-dated late Neogene carbonate platforms and margins: Sedimentary Geology, v. 175, p. 73-87.

Meyerhoff, A.A., and Hatten, C.W., 1974, Bahamas salient of North America: Tectonic framework, stratigraphy, and petroleum potential: American Association of Petroleum Geologists Bulletin, v. 58, p. 1201-1239.

Mylroie, J.E., 2008, Late Quaternary sea level position: Bahamian carbonate deposition and dissolution cycles: Quaternary International, v. 183, p. 61-75.

Pécheux, M., 1995, *Pseudorhapydionina moulladei*, a new large foraminifer of the Paleocene of Chiapas, south east Mexico: Revue de Micropaléontologie, v. 38, p. 169-176.

Pekar, S.F., and DeConto, R.M., 2006, High-resolution ice-volume estimates for the early Miocene: evidence for a dynamic ice sheet in Antarctica: Palaeogeography, Palaeoclimatology, Palaeoecology, v. 231, p. 101-109.

Pierson, B.J., 1982, Cyclic sedimentation, limestone diagenesis and dolomitisation in Upper Cenozoic carbonates of the southeastern Bahamas: PhD thesis, University of Miami, Florida, 286 p.

Robinson, E., and Wright, R.M., 1993, Jamaican Paleogene larger foraminifera, *in* Wright, R.M., and Robinson, E., eds., Biostratigraphy of Jamaica: Geological Society of America Memoir, v. 182, p. 283-342.

Schlager, W., 1999, Scaling of sedimentation rates and drowning of reefs and carbonate platforms: Geology, v. 27, p. 183-186.

Schlager, W., 2000, Sedimentation rates and growth potential of tropical, cool-water and mud-mound carbonate systems, *in* Insalaco, E., Skelton, P.W., and Palmer, T.J., eds., Carbonate Platform Systems: Components and Interactions: Geological Society, London, Special Publications, v. 178, p. 217-227.

Schlager, W., 2005, Carbonate sedimentology and sequence stratigraphy: SEPM Concepts in Sedimentology and Paleontology, v. 8, 200 p.

Serra-Kiel, J., Hottinger, L., Caus, E., Drobne, K., Ferrandez, C., Jauhri, A.K., Less, Gy., Pavlovec, R., Pignatti, J., Samsò, J.M., Schaub, H., Sirel, E., Strougo, A., Tambareau, Y., Tosquella, J., and Zakrevskaya, E., 1998, Larger foraminiferal biostratigraphy of the Tethyan Paleocene and Eocene: Bulletin de la Société Géologique de France, v. 169, p. 281–299.

Sirel, E., 2003, Foraminiferal description and biostratigraphy of the Bartonian, Priabonian and Oligocene shallow-water sediments of the southern and eastern Turkey: Revue de Paléobiologie, v. 22, p. 269-339.

Smout, A.H., and Eames, F.E., 1958, The genus Archaias (foraminifera) and its stratigraphical distribution: Palaeontology, v. 1, p. 207-225.

Stewart, B.W., Capo, R.C., and Chadwick, O.A., 1998, Quantitative strontium isotope models for weathering, pedogenesis and biogeochemical cycling: Geoderma, v. 82, p 173-195.

Still, W.C., Kahn, M., and Mitra, A., 1978, Rapid Chromatographic Technique for Preparative Separations with Moderate Resolution: The Journal of Organic Chemistry, v. 43, p. 2923-2925.

Vahrenkamp, V.C., Swart P.K., and Ruiz, J., 1991, Episodic dolomitisation of Late Cenozoic carbonates in the Bahamas: Evidence from Strontium isotopes. Journal of Sedimentary Petrology, v. 61, p. 1002–1014.

# PLATE 1
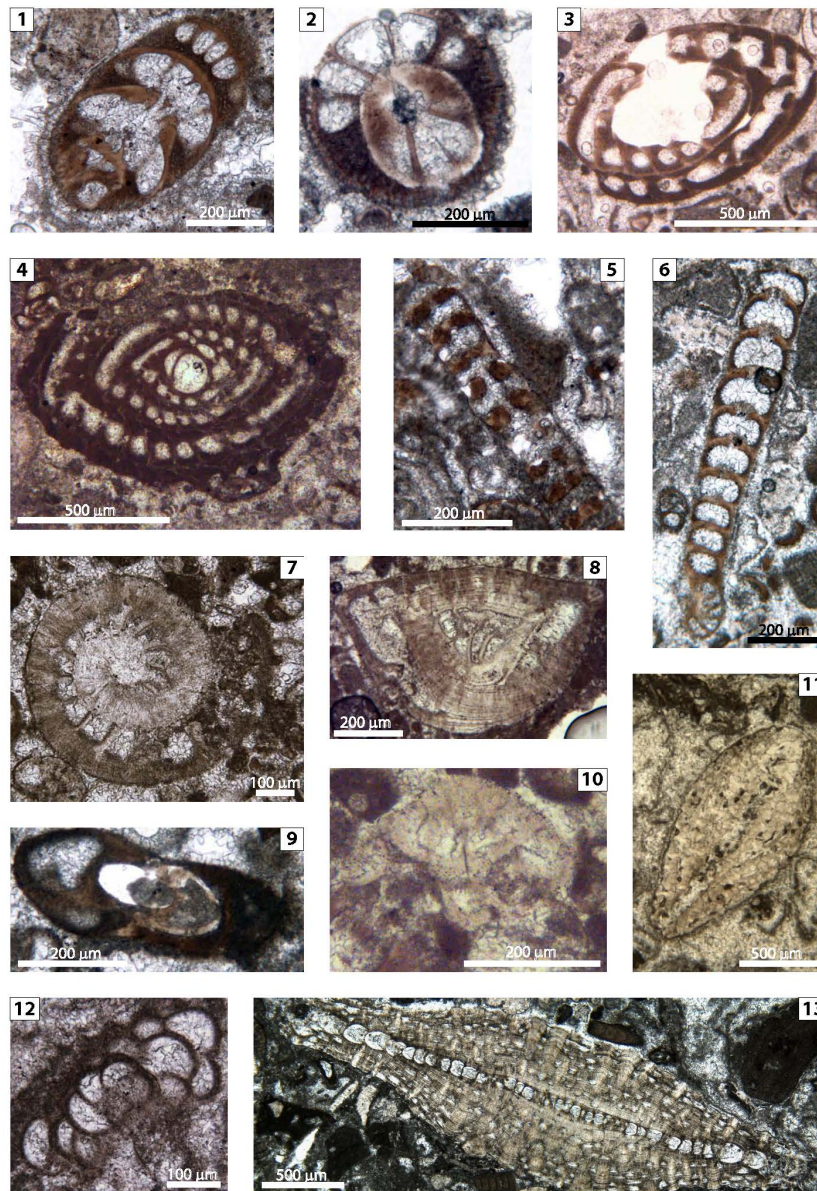


1. *Praerhapydionina delicata*, oblique section, scale = 200 μm.
2. *Praerhapydionina delicata*, transversal section, scale = 200 μm.
3. *Archaias* **cf.** *kirkukensis*, tangential-oblique section, scale = 500 μm.
4. *Archaias* **aff.** *operculiniformis*, oblique centered section, scale = 500 μm.
5. *Peneroplis* **aff.** *thomasi*, transversal section, scale = 200 μm.
6. *Spirolina cylindracea*, tangential subaxial section, scale = 200 μm.
7. *Neorotalia lithothamnica*, equatorial section, scale = 100 μm.
8. *Neorotalia lithothamnica*, subaxial section, scale = 200 μm.
9. *Dendritina* **sp.**, subaxial section, scale = 200 μm.
10. *Neorotalia viennoti*, axial section, scale = 200 μm.
11. *Miogypsina* **cf.** *intermedia*, subaxial section, scale = 500 μm.
12. *Planorbulina* **sp.**, random section, scale = 100 μm.
13. *Miolepidocyclina* **cf.** *burdigalensis*, subaxial section, scale = 500 μm.